

Published in final edited form as:

*Chem Commun (Camb)*. 2013 July 4; 49(52): 5823–5825. doi:10.1039/c3cc41072b.

## Vitamin-responsive Mesoporous Nanocarrier with DNA Aptamer-mediated Cell Targeting

Le-Le Li<sup>a,b,†</sup>, Mengying Xie<sup>a,‡</sup>, Jie Wang<sup>a</sup>, Xinyang Li<sup>a</sup>, Cheng Wang<sup>a</sup>, Quan Yuan<sup>a</sup>, Dai-Wen Pang<sup>a</sup>, Yi Lu<sup>b</sup>, and Weihong Tan<sup>c,d</sup>

Quan Yuan: yuanquan@whu.edu.cn; Dai-Wen Pang: dwpang@whu.edu.cn; Yi Lu: yi-lu@illinois.edu

<sup>a</sup>Key Laboratory of Analytical Chemistry for Biology and Medicine (Ministry of Education), College of Chemistry and Molecular Sciences, Wuhan University, Wuhan 430072, China

<sup>b</sup>Department of Chemistry, University of Illinois at Urbana-Champaign, Urbana, IL 61801, USA

<sup>c</sup>Department of Chemistry and Department of Physiology and Functional Genomics, Shands Cancer Center and UF Genetics Institute, Center for Research at the Bio/Nano Interface, University of Florida, Gainesville, Florida 32611-7200, United States

<sup>d</sup>State Key Laboratory for Chemo/Bio-Sensing and Chemometrics, College of Biology, and College of Chemistry and Chemical Engineering, Hunan University, Changsha 410082, China

### Abstract

A smart drug delivery system with cancer cell targeting and bioresponsive controlled drug release has been constructed by taking advantage of the protein-capped mesoporous nanovalve and a DNA aptamer.

A major challenge in current cancer therapeutics is the targeted delivery of cancer drugs into disease cells more efficiently while mitigate harmful side effects. This challenge is being met by the development of anti-cancer cell agents to achieve targeted drug delivery systems. Among them, anticell aptamers are single-stranded DNA or RNA molecules that can fold into a three-dimensional structure to bind with a certain type of cancer cells.<sup>1</sup> The high cell-binding affinity and selectivity, low immunogenicity, fast tissue penetration, rapid systemic clearance, and small size make aptamers excellent recognition elements for targeted delivery of therapeutics.<sup>2</sup>

In addition to targeting, the ability to induce triggerable delivery of anticancer drugs is another important factor to consider for the spatiotemporal control over the delivery of chemotherapeutic agents. Such “on-demand” controlled release systems could regulate the time and the site of drug delivery more precisely and thus increase drug retention in cancers. The ideal drug delivery systems will combine cancer cell targeting with subsequent intracellular triggerable controlled drug release to maximize cancer killing and minimize metastatic spread. Recently, mesoporous silica nanoparticles (MSNs) has received increasing attentions as nanocarriers for the controlled release of therapeutics due to their outstanding structural characteristics.<sup>3,4</sup> Despite the successes, internal stimuli used for the controlled-release systems and the mechanism by which the release is controlled are still

This journal is © The Royal Society of Chemistry

Correspondence to: Quan Yuan, yuanquan@whu.edu.cn; Dai-Wen Pang, dwpang@whu.edu.cn; Yi Lu, yi-lu@illinois.edu.

<sup>†</sup>These authors contributed equally to this work.

<sup>‡</sup>Electronic Supplementary Information (ESI) available: Experimental details and supplementary results. See DOI: 10.1039/b000000x/

limited. Furthermore, a main challenge for MSNs-based triggerable nanovalves is to achieve simultaneous targeting and drug release, which often requires coupling targeting group and capping group on the limited surface sites of the same nanoparticle.

Known as biotin as well as Coenzyme R, vitamin H is one of the B vitamin complex families, which acts as a growth promoter of all cells.<sup>5</sup> Recently, it has been shown that the vitamin H content in cancer cells is substantially higher than that in normal tissues.<sup>6</sup> Herein we report a novel method of taking advantages of different affinities of desthiobiotin and vitamin H toward avidin and combining targeting ability of aptamer to develop a new generation of MSNs-based nanovalves for simultaneous targeted drug delivery and intracellular triggerable drug release. As shown in Scheme 1, the MSN was selected as the inorganic scaffold to load with guest molecules, and the external surface was modified with desthiobiotin molecules. Then the pores were capped by avidin proteins through strong desthiobiotin-avidin interaction. Furthermore, a cancer cell-specific DNA aptamer was attached to the avidin on the surface of MSNs to result in the final nanocarriers. Due to selective targeting ability of the aptamers on the surface of MSN-Avi-Apt, the loaded nanocarriers can specifically target and then enter cancer cells through receptor-mediated endocytosis. Since the pores of MSN-Avi-Apt are capped, there is less premature leakage of drugs during the delivery process. Upon entering the target cancer cells, MSN-Avi-Apt will be uncapped by intracellular vitamin H biomolecules, accelerating the release of drugs from nanocarriers and the killing of target cancer cells.

The prepared MSNs (ca. 150 nm) with a typical hexagonal channel-like mesoporous structure were confirmed by TEM, SEM, X-ray diffraction and nitrogen adsorption-desorption isotherms (Fig. S1–S4). The outlet of mesoporous silica was modified with amine groups and then conjugated with desthiobiotin molecules through EDC/sulfo-NHS coupled reactions. The efficient attachment of desthiobiotin onto MSNs was validated by the appearance of the broad absorption band at around  $1680\text{ cm}^{-1}$  in the FTIR spectroscopy that can be assigned to vibrations of the cyclic-urea group within the attached desthiobiotin molecules (Fig. S5). For preparation of the gated material (MSN-Avi), avidin was added to cap the pores through the formation of desthiobiotin-avidin complex (Fig. S1a). To simultaneously provide cancer-targeting capability to the avidin-capped MSNs, we chose a 26-mer DNA aptamer sgc8 as the targeting aptamer for the further functionalization. The sgc8 has been shown to be highly specific to binds to cell membrane receptor protein tyrosine kinase 7 (PTK 7),<sup>7</sup> a protein that is over expressed on the plasma membrane of CCRF-CEM cells (CEM), a human precursor T-cell acute lymphoblastic leukemia (T-ALL) cell line.<sup>8</sup> In addition, the sgc8 aptamer was labeled with a desthiobiotin group at the 5'-end to allow attaching onto the avidins on the surface of MSN-Avi to give final nanocarriers MSN-Avi-Apt. Zeta potential measurements (Fig. S6) showed that the MSN-Avi-Apt were highly negatively charged. The amount of DNA conjugation was determined to be  $0.4\text{ }\mu\text{mol/g SiO}_2$  based on UV/Vis spectroscopy.

The intracellular release of the entrapped drugs is related to a highly effective displacement reaction involving the presence of vitamin H biomolecules in the cancer cells (Fig. 1a). The association constant ( $K_a$ ) of vitamin H toward avidin ( $\sim 1 \times 10^{15}\text{ M}^{-1}$ )<sup>9,10</sup> is  $\sim 20$ -fold higher than that for desthiobiotin to avidin molecules ( $5 \times 10^{13}\text{ M}^{-1}$ ),<sup>11</sup> which is the working principle of our vitamin-responsive nanovalves through effective dissociation reaction by displacement. To investigate the target-triggered controlled release property of the ensemble, rhodamine 640 (denoted as Rh640) that used as a model guest molecule was loaded into the pores of MSN-Avi-Apt. The uncapping and subsequent release of the dye was monitored through the measurement of the absorbance maximum of Rh640 (553 nm) in solution as a function of time. As shown in Fig. 1b, the nanogated nanocarriers exhibited a negligible leakage of the entrapped dye molecules during the first 2 h in the absence of

target, thus indicating the good end-capping efficiency. When vitamin H molecules were added to the suspension, a fast release of dye molecules occurred due to the effective competitive binding. Interestingly, the release curve shows a fairly slow release for the first 100 min after the addition of vitamin H. This result can be explained by the replace reaction process, in which four vitamin H molecules bind with one capped avidin for the effective uncapping. After 100 min, the capping proteins are effectively replaced, leading to a faster release of Rh 640. This release curve compares well with the feather of reported protein-capped MSNs system.<sup>4b</sup> In contrast, only slight leaking of dye molecules (less than 10%) from the nanogated nanocarriers occurred even after 10 h incubation without vitamin H exposure, demonstrating the stable capping capability of the nanovalves.

To test the targeting specificity of the nanocarriers, we incubated MSN-Avi and MSN-Avi-Apt with CEM cells at 37 °C for 2 h. Subsequent analysis using confocal microscopy (Fig. 2a) revealed that CEM cells incubated with MSN-Avi-Apt bearing *sgc8* aptamer showed strong fluorescence within the cancer cells, while the nanocarriers MSN-Avi without aptamer attachment gave rise to less fluorescence in the CEM cells (Fig. 2b), confirming the role of the specific aptamer in cell binding and endocytosis-based internalization mechanism. To further confirm the aptamer-mediated targeting specificity, we performed similar experiments by using Ramos cells with no receptor protein PTK 7 on the membrane as control cancer cells. Both MSN-Avi-Apt and MSN-Avi exhibit much less capability of cell-binding and internalization to Ramos cells (Fig. 2c and Fig. S7), thus showing that the aptamer-modified nanocarriers have negligible binding affinity to the non-target cells. The targeting specificity of the aptamer *sgc8* toward CEM cells was also confirmed by flow cytometry assays of the cells treated with a 6-carboxyfluorescein (FAM)-labeled *sgc8* (Fig. S8). As shown in Fig. 2d and 2f, a 6-fold increase in mean fluorescence intensity was observed for CEM cells treated with the FAM-labeled MSN-Avi-Apt compared to the negative controls, but no obvious change was observed for Ramos cells (Fig. 2e and 2g).

The *in vitro* cytotoxicities of the DOX-loaded nanocarriers were tested through MTT assay to evaluate their anti-cancer potential. Both cell lines treated with MSN-Avi or MSN-Avi-Apt alone showed negligible cell death even at the concentration of 200 µg/mL (Fig. S9), indicating excellent biocompatibility of the nanocarriers. The loading content of DOX in MSN-Avi-Apt was found to be 1.7%. The DOX-loaded MSN-Avi-Apt also shows a vitamin-responsive drug release behavior (Fig. S10). As shown in Fig. 3, DOX-loaded MSN-Avi-Apt showed significantly higher cytotoxicity to CEM cells as compared to DOX-loaded MSN-Avi and DOX alone. The cell viabilities were  $32.7 \pm 6\%$  (mean  $\pm$  SD) for CEM cells treated with DOX-loaded MSN-Avi-Apt at DOX concentration of 5 µg/ml, while the cell viabilities were  $65.6 \pm 6\%$  and  $60.8 \pm 4\%$  for cells treated with DOX-loaded MSN-Avi and DOX alone at the same concentrations, respectively. The low cytotoxicity of DOX-loaded MSN-Avi is likely due to inefficient cellular uptake, which compared well with the cellular internalization studies. In contrast to the dramatic enhancement in cytotoxic effects for MSN-Avi-Apt to the CEM cells, a much less pronounced cytotoxicity of the MSN-Avi-Apt to the Ramos cells (cellular viability:  $67.4 \pm 4\%$ ,  $73.7 \pm 2\%$ , and  $74.9 \pm 4\%$  for three samples with the DOX concentration of 5 µg/mL respectively) was observed. Based on these data from the MTT assay, one can draw the conclusion that improved and selective cytotoxicity to target cancer cells can be achieved for the current smart nanocarriers, which can be attributed to three possible reasons: (1) the aptamer-functionalization enables the nanovalves bind to and be internalized by CEM cells selectively, (2) the capping of the pores can alleviate the premature leakage of highly toxic anticancer drugs during the targeting process, (3) intracellular vitamin H-triggered drug release of the encapsulated drugs improves antiproliferative activity in cancer cells. Since the MSN-Avi-Apt was highly negatively charged, it is reasonable that the nanocarriers are able to escape from the endosome and to interact with the vitamin in cytoplasm.<sup>12</sup>

In conclusion, we demonstrate a smart drug delivery system with efficient cancer-specific delivery and intracellular controlled release of the drug. The sgc8 aptamer serves as a model system to be conjugated on the MSN-based nanovalves for targeting specific cancer cell, while the pores were capped by the desthiobiotin-avidin complex to eliminate the premature drug leakage before they reach the specific sites. The vitamin H endows the opening of the nanovalves for intracellular controlled release of the entrapped drugs. The efficient cancer-cell-specific drug delivery of the nanovalves demonstrated a significant enhancement in the anticancer activity.

## Supplementary Material

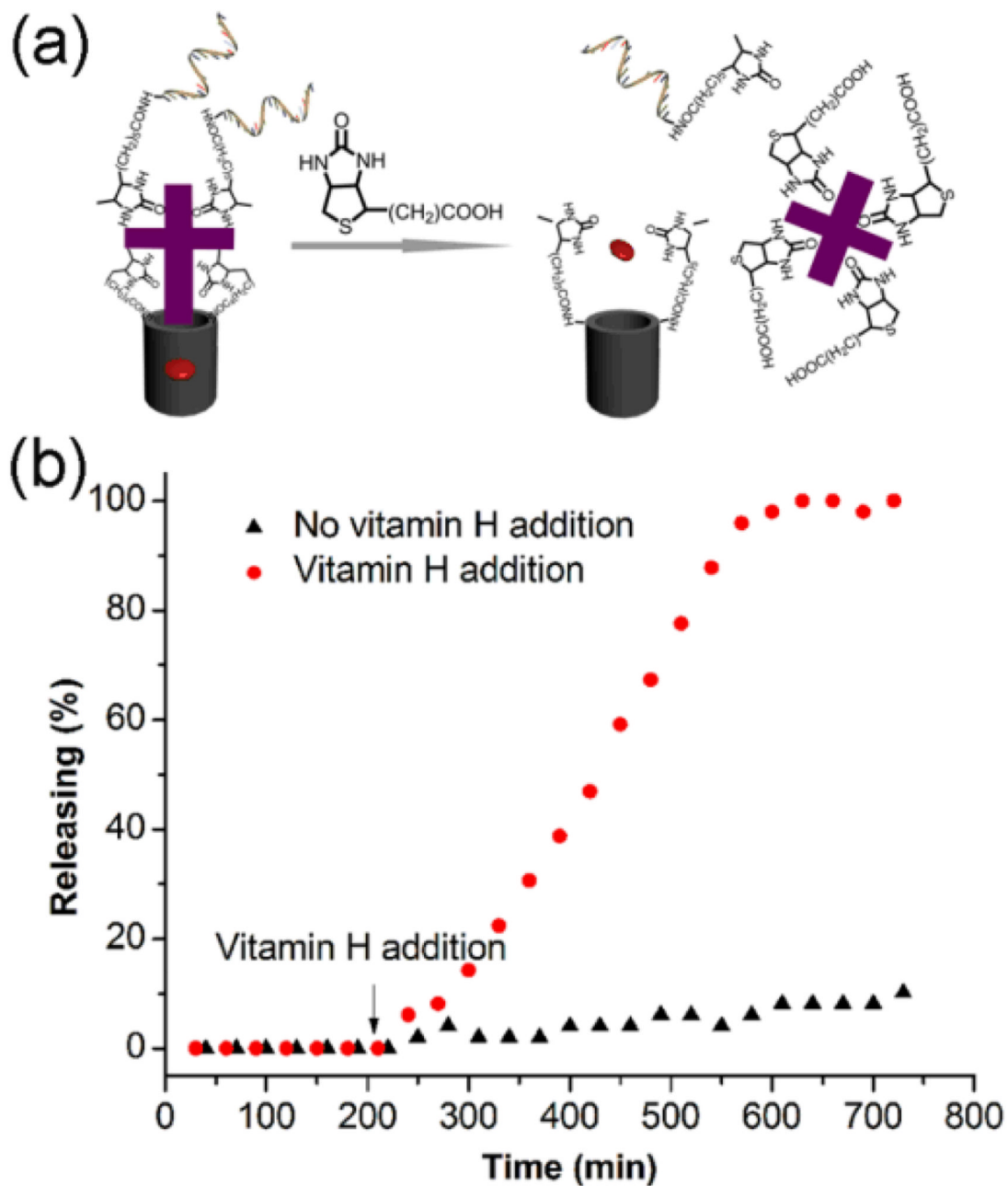
Refer to Web version on PubMed Central for supplementary material.

## Acknowledgments

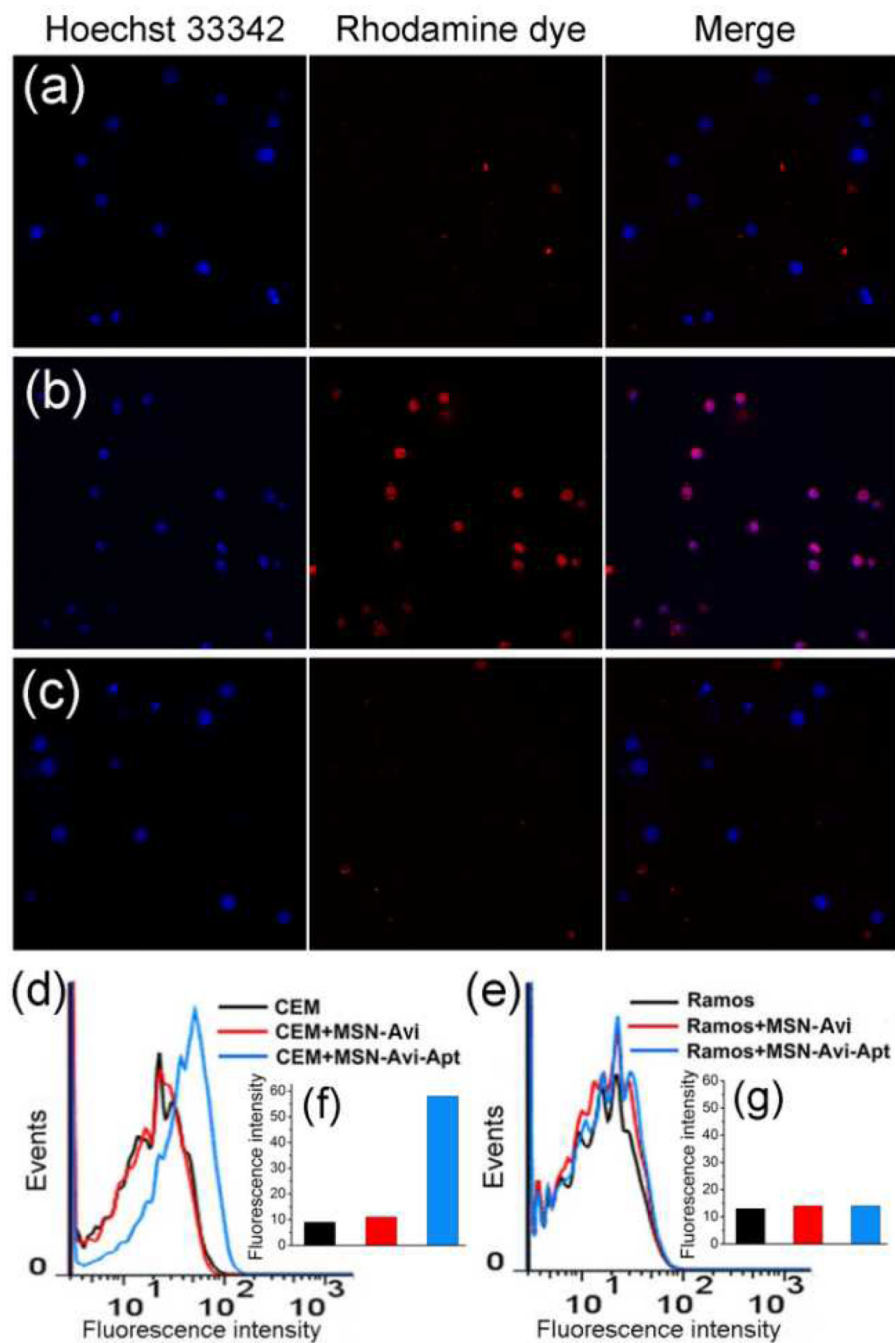
This work was supported by the National Natural Science Foundation of China (21201133, 51272186 to QY) and the U.S. National Institutes of Health (Grant ES016865 to YL). Q. Yuan thanks Wuhan University for start-up funds and large-scale instrument and equipment sharing foundation.

## Notes and references

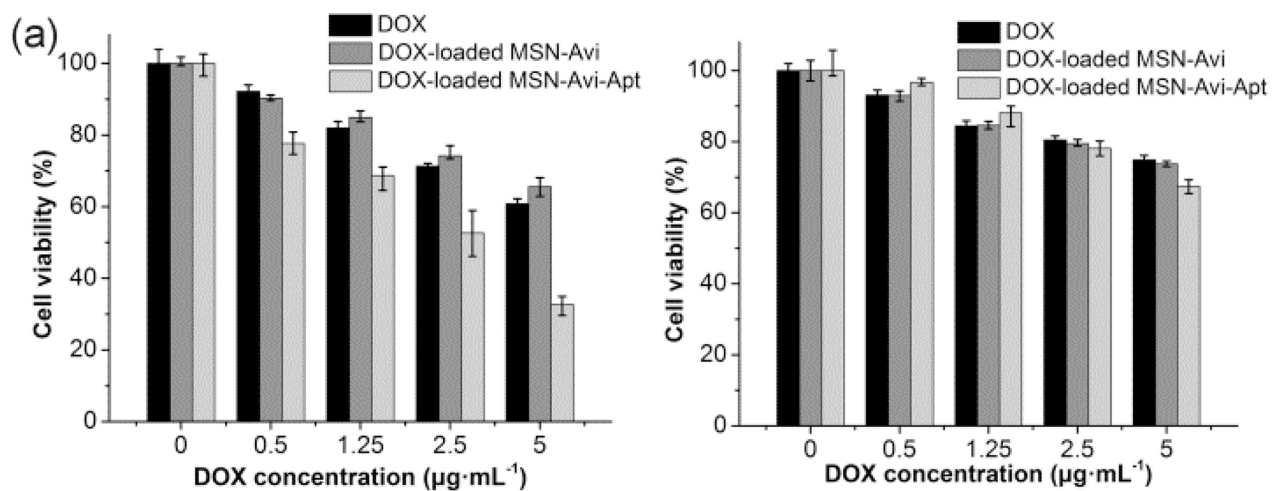
1. Tuerk C, Gold L. *Science*. 1990; 249:505. [PubMed: 2200121] Ellington AD, Szostak JW. *Nature*. 1990; 346:818. [PubMed: 1697402] Fang X, Tan W. *Acc. Chem. Res.* 2010; 43:48. [PubMed: 19751057]
2. Xing H, Wong NY, Xiang Y, Lu Y. *Curr. Opin. Chem. Biol.* 2012; 16:429. [PubMed: 22541663]
3. Vallet-Regí M, Balas F, Arcos D. *Angew. Chem. Int. Ed.* 2007; 46:7548. Yang P, Gai S, Lin J. *Chem. Soc. Rev.* 2012; 41:3679. [PubMed: 22441299]
4. Vivero-Escoto JL, Slowing II, Wu C-W, Lin VS-Y. *J. Am. Chem. Soc.* 2009; 131:3462. [PubMed: 19275256] Schlossbauer A, Kecht J, Bein T. *Angew. Chem. Int. Ed.* 2009; 48:3092. Croissant J, Zink JJ. *J. Am. Chem. Soc.* 2012; 134:7628. [PubMed: 22540671]
5. Bowman BB, Rosenberg IH. *J. Nutr.* 1987; 117:2121. [PubMed: 3694289]
6. Russell-Jones G, McTavish K, McEwan J, Rice J, Nowotnik D. *J. Inorg. Biochem.* 2004; 98:1625. [PubMed: 15458825]
7. Mossie K, Jallal B, Alves F, Sures I, Plowman GD, Ullrich A. *Oncogene*. 1995; 11:2179. [PubMed: 7478540]
8. Shanguan D, Li Y, Tang Z, Cao ZC, Chen HW, Mallikaratchy P, Sefah K, Yang CJ, Tan W. *Proc. Natl. Acad. Sci. USA*. 2006; 103:11838. [PubMed: 16873550]
9. Müller W, Ringsdorf H, Rump E, Wildburg G, Zhang X, Angermaier L, Knoll W, Liley M, Spinke J. *Science*. 1993; 262:1706. [PubMed: 8259513]
10. Florin E-L, Moy VT, Gaub HE. *Science*. 1994; 264:415. [PubMed: 8153628]
11. Hoffmann M, Müller W, Ringsdorf H, Rourke AM, Rump E, Suci PA. *Thin Solid Films*. 1992; 210/211:780.
12. Slowing I, Trewyn BG, Lin VS-Y. *J. Am. Chem. Soc.* 2006; 128:14792. [PubMed: 17105274]



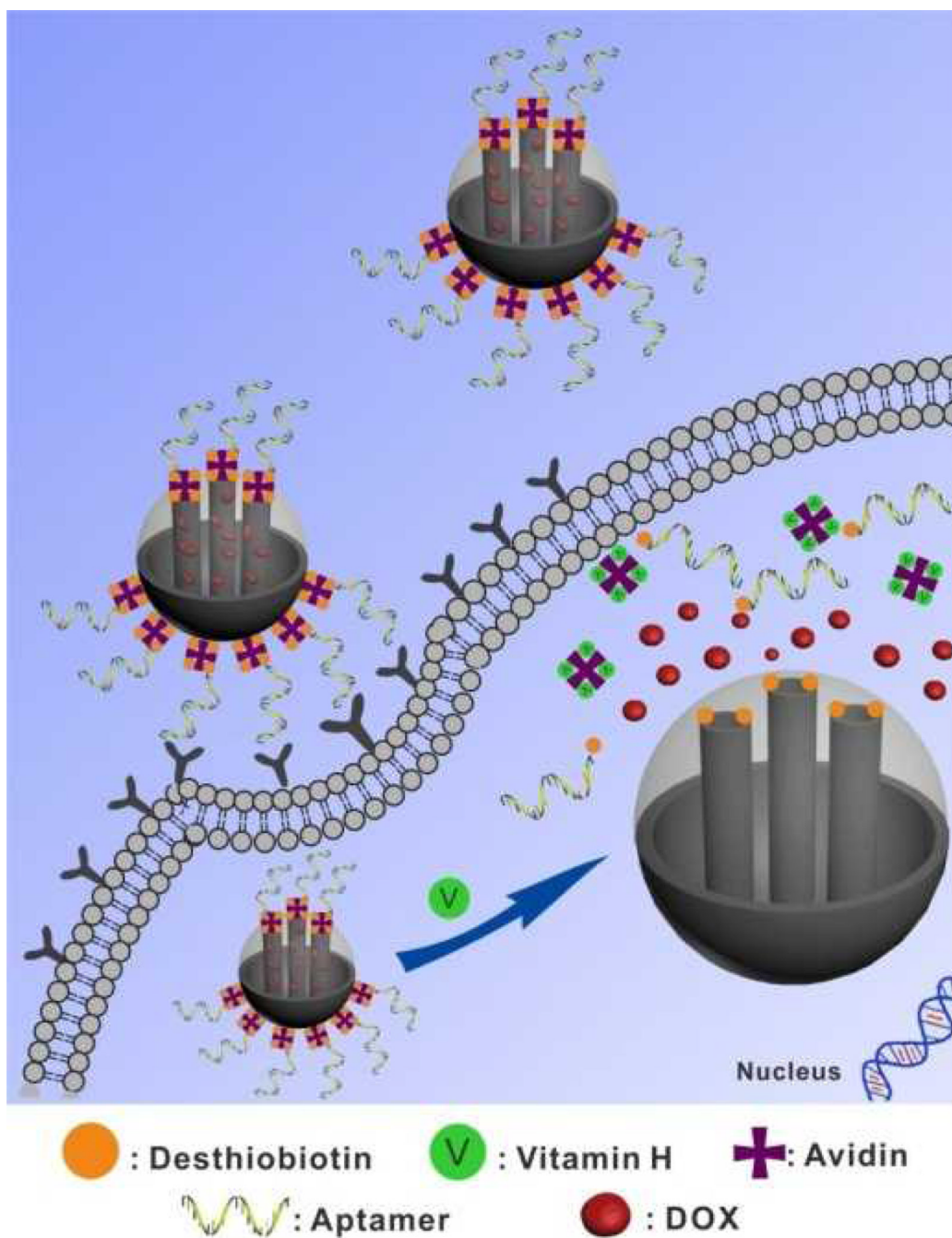
**Fig. 1.** (a) Schematics of vitamin-responsive drug release process for the nanovalves. (b) Release curve for MSN-Avi-Apt with and without vitamin H addition. Data have been normalized to the maximum level of dye released in the experiment.



**Fig. 2.** Confocal microscopy images of (a) CEM cells treated with MSN-Avi, (b) CEM cells treated with MSN-Avi-Apt, and (c) Ramos cells treated with MSN-Avi-Apt. Flow cytometry analysis to monitor the binding of MSN-Avi-Apt and MSN-Avi with (d) CEM cells and (e) Ramos cells. Inset shows the corresponding histograms of the flow cytometric results of (f) CEM cells and (g) Ramos cells, respectively.



**Fig. 3.** Cytotoxicity assay of (a) CEM cells (target cells) and (b) Ramos cells (control cells) treated with DOX, DOX-loaded MSN-Avi, and DOX loaded MSN-Avi-Apt.



**Scheme 1.**  
Schematic Illustration of Vitamin-responsive Release System for Targeted Cancer Therapy Guided by Aptamer.